



# Spatial variability and radiation assessment of the radionuclides in soils and sediments around a uranium tailings reservoir, south of China

Yuanyuan Liu<sup>1,2,3</sup> · Weibo Zhou<sup>1,3</sup> · Haiyan Liu<sup>2</sup> · Qianglin Wei<sup>2</sup> · Bai Gao<sup>2</sup> · Gongxin Chen<sup>2</sup>

Received: 16 August 2019 / Published online: 11 March 2020  
© Akadémiai Kiadó, Budapest, Hungary 2020

## Abstract

The concentrations of  $^{238}\text{U}$ ,  $^{226}\text{Ra}$ ,  $^{232}\text{Th}$  and  $^{40}\text{K}$  and gross  $\alpha$ ,  $\beta$  were measured in soils and sediments around a uranium tailings reservoir to analyze the distribution of radionuclides and evaluate radiation impacts. Results showed that the highest concentrations of  $^{238}\text{U}$ ,  $^{226}\text{Ra}$  and  $^{232}\text{Th}$  occurred in the tailings sand, while the highest concentrations of  $^{40}\text{K}$  in the farmland. Nuclides concentrations and radioactivity levels decreased with distance away from the reservoir area. Moreover, the calculated gamma absorbed dose rates varied from 54 to 5369 nGy h<sup>-1</sup> in study area. The average absorbed dose rate was approximately 52 times higher than the national average value in the tailings reservoir, but it reduced to about twice in the sediments downstream.

**Keywords** Radiation assessment · Soil and sediment · Radionuclide variability · Uranium tailings reservoir · Critical zones

## Introduction

Rapid development of nuclear energy leads to an enhanced exploitation of uranium ore, which results in serious soil contamination and environmental problems [1]. During the uranium mining and smelting, a large number of low-grade waste rocks and slags are produced, and are piled up in the mine area and tailings reservoir for a long time. It is reported that more than 4000 uranium mines occur worldwide [2, 3], which produce about  $9.38 \times 10^8 \text{ m}^3$  of uranium tailings. In China, there are more than 150 storage sites of solid wastes including uranium tailings waste rocks [4]. Radionuclides are released into the soil and water environment by rainfall leaching and infiltration in the stacked tailings and waste rocks, which poses great risks to surrounding ecological

environment. Therefore, extensive surveys on radiation in abandoned uranium mines have received particular attention worldwide.

A wide variety of radioactive substances have been found in uranium mine areas. Their concentrations are usually more than 2–3 orders of magnitude higher than their natural background values. The radionuclides contain a series of long-lived radionuclides, such as uranium ( $^{238}\text{U}$ ), radium ( $^{226}\text{Ra}$ ) and thorium ( $^{232}\text{Th}$ ). Many studies on the radioactivity levels in soil [5–8], vegetation and plants [5, 9–11], water bodies [12–15] and sediments [16, 17] around uranium mines have been performed. Results showed that uranium could be transferred from mine tailings to the contaminated creek branch over time, which was further confirmed by isotopic composition in waters, sediment leachates and bulk sediments [18]. Uranium contamination and its risks increased with distance approaching the uranium tailings reservoir [19]. Gamma absorbed dose rate and radiation dose of a uranium mine in India and a Gold Mine in South Africa were estimated to be far above the permissible value set by the World Health Organization (WHO 2008) [20]. Déjeant et al. [21] investigated the evolution of uranium distribution and speciation in mill tailings from the COMINAK mine (Niger). Kayzar et al. [18] suggested that adsorption was a key factor of transfer along the creek between sediment surfaces and bulk sediment. Correlation analysis helps to

✉ Weibo Zhou  
zwbzyz823@163.com

<sup>1</sup> School of Water and Environment, Chang'an University, No. 126 Yanta Road, Xi'an 710054, China

<sup>2</sup> School of Water Resources and Environmental Engineering, East China University of Technology, No 418. Guanglan Road, Nanchang 330013, China

<sup>3</sup> Key Laboratory of Subsurface Hydrology and Ecological Effect in Arid Region of Ministry of Education, Chang'an University, No. 126 Yanta Road, Xi'an 710054, China

identify the source and relationship of nuclides. Yan and Luo [7] suggested that concentrations of  $^{232}\text{Th}$  were significantly correlated with those of  $^{226}\text{Ra}$ , and the concentrations of  $^{226}\text{Ra}$  and  $^{40}\text{K}$  were significantly correlated. Radionuclides distribution showed a profound influence on soil properties and microbial diversity in the uranium mill tailing. Chautard et al. [22] found good correlations between facies, granulometry, U concentration and  $^{226}\text{Ra}$  activity.

Researches on long-lived natural radioactive nuclides  $^{238}\text{U}$ ,  $^{226}\text{Ra}$ ,  $^{232}\text{Th}$  and  $^{40}\text{K}$  are helpful in identifying the sources and the radiation impact of tailings reservoir. Over the past decades, extensive research projects focusing on uranium tailings reservoir have been carried out, but relatively few work has reported on the spatial variability of the radionuclides considering both soil and sediment samples around a uranium tailings reservoir. These radionuclides emit  $\alpha$ ,  $\beta$  and  $\gamma$  rays, and the gross  $\alpha/\beta$  activity can reflect the radioactivity level in a region. Thus, it is necessary to measure gross  $\alpha$  and  $\beta$  activity in the soils of uranium tailings reservoir area for the environmental impact assessment. In addition, the external absorbed dose rates of radioactive nuclides in the tailings reservoir can evaluate the radiation effect on the surrounding residents. The external gamma absorbed dose rates in air generally exhibits a high background level in the uranium mine. Surface and ground water flow and geochemistry of underlying sediments are likely important factors affecting nuclide migration.

Therefore, the objectives of this investigation are to: (1) characterize the activity concentrations of radionuclides  $^{238}\text{U}$ ,  $^{226}\text{Ra}$ ,  $^{232}\text{Th}$  and  $^{40}\text{K}$  and gross  $\alpha$ ,  $\beta$  in soils and sediments samples collected from the tailings reservoir, dam, the upstream and downstream channels and the farmland around the uranium tailings reservoir; (2) assess public health radiation impact with  $\gamma$  absorption dose rate; (3) identify a radiological baseline for this study area; (4) provide basic data for a study of radionuclide migration mechanism in the soil–water system around uranium tailings reservoir.

## Materials and methods

### Description of the study area

The uranium mine is located in Jiangxi province in south part of China. It is a volcanic rock type uranium mine. A uranium tailings reservoir that formed since more than 60 years ago is located in the eastern of uranium mine. A large amount of tailings are stored in the reservoir. The uranium tailings reservoir is surrounded by mountains on three sides, being like a valley. The farmland is in the opposite direction of the tailings dam. The area belongs to subtropical humid and rainy climate, with abundant sunshine and abundant rainfall. The average annual temperature is 18.1 °C

with extreme low temperature of  $-5.9$  °C and extreme high temperature of 39.9 °C. The surface water systems are well-developed and many rivers run across. The leachate in the uranium tailings reservoir seeps from the bottom of tailings dam and flows into the river.

### Sample collection and pretreatment

The study area and sampling location are shown in Fig. 1. Total 29 samples were collected from 5 different regions around uranium tailings. These include 10 samples from tailings sand, 6 samples from tailings dam soil, 10 samples from surface sediments of upstream and downstream of channel, and 3 samples from farmland soil. The soil samples were taken from 5 cm below land surface and sediment samples were taken from the surface of bottom mud, and then were stored in closed plastic packaging bags with corresponding labels. The geographical location of each sample site was recorded by GPS. The samples were taken back to Chemical Analysis and Physical Testing Center of East China University of Technology for sample processing and measurement.

Sample pretreatment as well as collection were carried out in strict accordance to GB/T 11743-2013 “Determination of radionuclides in soil by gamma spectrometry” [23]. In laboratory, the samples were ground until the thickness of the grains became to less than 0.15 mm and were dried in an oven at 100 °C for 24 h to ensure that moisture was completely removed. The samples were weighed, packed in polyethylene cylindrical beakers and sealed to prevent the escape of radon. The weighed and tightly sealed samples were left for at least 4 weeks to reach secular equilibrium between  $^{226}\text{Ra}$  and  $^{222}\text{Rn}$  as well as their daughters (mostly  $^{214}\text{Bi}$  and  $^{214}\text{Pb}$ ).

### Radioactivity measurements and estimation

The activity concentrations of  $^{238}\text{U}$ ,  $^{226}\text{Ra}$ ,  $^{232}\text{Th}$  and  $^{40}\text{K}$  were measured using low background HPGe semiconductor detector (ORTEC GMX40P) with energy resolution of 2.1 keV at gamma ray energy of 1332 keV of  $^{60}\text{Co}$ . The gamma spectra were recorded and analyzed with MAESTRO-32 software. The activity concentration of  $^{238}\text{U}$  was determined via its daughter  $^{234}\text{Th}$  (92.6 keV), and  $^{226}\text{Ra}$  was determined via  $^{214}\text{Pb}$  (351.9 keV) and  $^{214}\text{Bi}$  (609.3 keV, 1120.3 keV), whereas  $^{232}\text{Th}$  was determined by  $^{208}\text{Tl}$  (583.4 keV) and  $^{228}\text{Ac}$  (911.2 keV); concentrations of  $^{40}\text{K}$  were determined with emission line 1460.8 keV [18].

According to the relative method [24], the ratio of the characteristic peak net count rate of the sample to the activity is equal to the ratio of the standard source net count rate to its activity, as shown in formula (1):

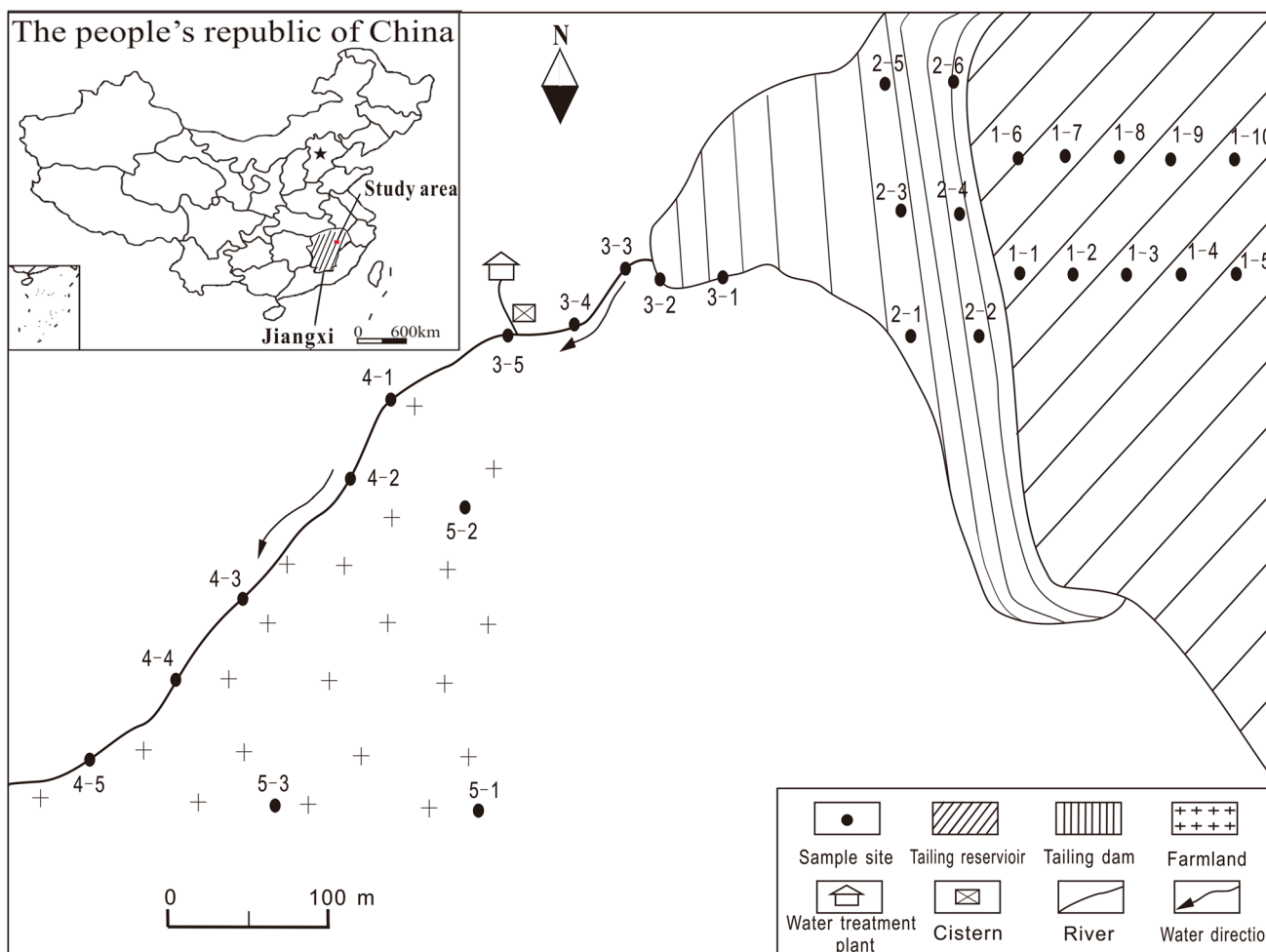


**Fig. 1** Situations of sampling points in the study area (the 10 samples in the tailings sands were at 1-1...1-10; 6 samples in the tailings dam soils were at 2-1...2-6; 5 samples in the sediments of upstream channel were at 3-1...3-5; 5 samples in the sediments of downstream channel were at 4-1...4-5; and 3 samples in the farmland soil were at 5-1...5-3)

$$\frac{(N_s/t_s - N_b/t_b)}{(N_0/t_0 - N_b/t_b)} = \frac{A_s}{A_0} \tag{1}$$

where,  $N_s$  and  $N_0$  are the gross counts of characteristic peak of the sample and standard source, respectively;  $A_s$  and  $A_0$  represent the corresponding activity concentration ( $Bq\ g^{-1}$ ) of the sample and standard source, respectively;  $N_b$  is background counts corresponding characteristics of the energy;  $t_s$ ,  $t_0$  and  $t_b$  is the measurement time of the sample, standard source and background, respectively. The expanded  $2\sigma$  uncertainty ranges are 3.21–3.59%, 3.28–5.50%, 3.23–3.30% and 3.32–3.50% for  $^{238}U$ ,  $^{226}Ra$ ,  $^{232}Th$  and  $^{40}K$  concentrations measurements, respectively. They all meet the requirements of GBT11743-2013 ( $^{238}U$  less than 20%,  $^{226}Ra$  and  $^{232}Th$  and  $^{40}K$  less than 10%).

The gross  $\alpha$  and  $\beta$  activity concentrations in soils were measured by the relative method using four-channel low

background  $\alpha/\beta$  measuring instrument (FYFS-400X). The instrument was calibrated according to GB/T 11682-2008 “low background alpha and/or beta measuring instruments” [25]. The detection efficiency was calibrated by  $^{241}Am$  and KCl powder standard source (purchase in National Institute of Metrology, China). The test results of four channels detection efficiency were 10–13% for  $\alpha$  and 35–42% for  $\beta$ , which are sufficient to meet the requirements of measurement.

Some 160 mg (same as the  $^{241}Am$  and KCl standard source) soil sample powder were weighed and laid in the  $\phi$  45 mm stainless steel sample tray. A few drops of anhydrous ethanol were added for mixing evenly. After ethanol evaporation, the samples were transferred into the measuring instrument for determination of  $\alpha$  and  $\beta$  activity concentrations. Each sample measurement ran 10 times with once of 3600 s.

The gross  $\alpha$  and  $\beta$  activity concentrations for the solid samples was calculated by formula (2):

$$A_{\alpha,\beta} = \frac{R_x - R_0}{R_s - R_0} \times A_s \quad (2)$$

where  $A_{\alpha,\beta}$  is  $\alpha$  or  $\beta$  activity concentration of soil sample,  $\text{Bq g}^{-1}$ ;  $R_x$ ,  $R_0$  and  $R_s$  are the gross counting rate of sample, background and standard source, respectively,  $\text{s}^{-1}$ ;  $A_s$  is the activity concentration of standard source ( $^{241}\text{Am}$  for  $\alpha$ ,  $10.3 \text{ Bq g}^{-1}$  and  $\text{KCl}$  for  $\beta$ ,  $14.5 \text{ Bq g}^{-1}$ ).

The natural radiation is mainly caused by the  $^{238}\text{U}$ ,  $^{232}\text{Th}$  and  $^{40}\text{K}$  series radionuclides. The Beck formula method [26] was used to calculate the external gamma radiation air absorption dose rates ( $D_\gamma$ ) at 1.0 m above ground using the activity concentrations (Eq. 3).

$$D_\gamma = k_U \times A_U + k_{Th} \times A_{Th} + k_K \times A_K \quad (3)$$

where  $k_U$ ,  $k_{Th}$ , and  $k_K$  are the absorbed dose rate conversion factors for  $^{40}\text{K}$ ,  $^{238}\text{U}$  and  $^{232}\text{Th}$  ( $\text{nGy h}^{-1}/(\text{Bq kg}^{-1})$ ), respectively;  $A_K$ ,  $A_U$  and  $A_{Th}$  are the activity concentrations for  $^{40}\text{K}$ ,  $^{238}\text{U}$  and  $^{232}\text{Th}$ , respectively.  $k_K = 0.0417 \text{ (nGy h}^{-1})/(\text{Bq kg}^{-1})$ ;  $k_U = 0.462 \text{ (nGy h}^{-1})/(\text{Bq kg}^{-1})$ ;  $k_{Th} = 0.604 \text{ (nGy h}^{-1})/(\text{Bq kg}^{-1})$  [27].

## Results and discussion

### Distribution of $^{238}\text{U}$ , $^{226}\text{Ra}$ , $^{232}\text{Th}$ and $^{40}\text{K}$

The radionuclide activity concentrations in soil samples are presented in Table 1. The data of Jiangxi province were used as the background value [28], and the national average data [29] were used as reference values for analysis. As can be seen from Table 1,  $^{226}\text{Ra}$  had the highest concentration in samples around the tailings reservoir, followed by  $^{238}\text{U}$  and  $^{232}\text{Th}$ . Comparing the concentrations of the four nuclides in samples from different regions (e.g. the tailings reservoir, dam, channel sediment and farmland area), it can be seen that the highest concentrations of  $^{238}\text{U}$ ,  $^{226}\text{Ra}$  and  $^{232}\text{Th}$

occurred in the tailings sand, while  $^{40}\text{K}$  showed the highest concentration in the farmland. It indicates that nuclides concentrations changed substantially in different regions around the tailings reservoir.

Concentrations of  $^{238}\text{U}$ ,  $^{226}\text{Ra}$  and  $^{232}\text{Th}$  in the tailings sand ranged from  $3.70$  to  $10.54 \text{ Bq g}^{-1}$ ,  $7.68$  to  $14.42 \text{ Bq g}^{-1}$  and  $0.44$  to  $0.81 \text{ Bq g}^{-1}$ , respectively, which are comparable to the values of tailings sand samples in a previous study [30]. But the average concentrations of  $^{238}\text{U}$ ,  $^{226}\text{Ra}$  and  $^{232}\text{Th}$  were significantly higher than the background value and the national average value. It indicates that there is radioactive residue in the tailings sand, which may result from inadequate hydrometallurgy and long-term sedimentation involving the effluent.  $^{226}\text{Ra}$  had the highest concentrations in tailings sand with a mean value being 210 times of the background value, and 4 times of the sediment of upstream channel. Such high levels of  $^{226}\text{Ra}$  may be attributed to uranium hydrometallurgy process, where 99%  $^{226}\text{Ra}$  of the ore are present in the tailings with only 1% entering the solution [31]. The average concentration of  $^{238}\text{U}$  in tailings sand was 111 times of the background value, and 164 times of the national average.

Concentrations of  $^{232}\text{Th}$  in the dam samples were similar to the natural background levels. The distribution of the four radionuclides in the dam was relatively uniform, although the radioactivity concentrations were significantly lower than other sites around the tailings reservoir. This may be due to that the dam is built on granite bedrock where the topsoil is exogenous.

Average concentrations of  $^{238}\text{U}$ ,  $^{226}\text{Ra}$  and  $^{232}\text{Th}$  in the sediments of upstream channel were 3.9, 47.4 and 3.7 times of the background value, respectively. The high concentrations indicate that the sediments in the channel are affected by the deposition of radionuclides in the leachate from the tailings reservoir. The sediments in the channel receives discharge effluents containing radionuclides from the leaching in the tailings waste. Although the nuclides in the sediments of upstream channel were much higher than the background

**Table 1** The statistics of radionuclides activity concentrations in soil and sediment samples ( $\text{Bq g}^{-1}$ )

Sample location	$^{238}\text{U}$		$^{226}\text{Ra}$		$^{232}\text{Th}$		$^{40}\text{K}$	
	Range	Average $\pm$ SD	Range	Average $\pm$ SD	Range	Average $\pm$ SD	Range	Average $\pm$ SD
Tailings sand (n=10)	3.70–10.54	6.22 $\pm$ 2.24	7.68–14.42	11.13 $\pm$ 2.15	0.44–0.81	0.65 $\pm$ 0.12	0.14–0.51	0.24 $\pm$ 0.14
Dam (n=6)	0.02–0.46	0.22 $\pm$ 0.16	0.06–0.77	0.22 $\pm$ 0.27	0.04–0.17	0.08 $\pm$ 0.05	0.07–0.37	0.20 $\pm$ 0.11
upstream channel (n=5)	0.38–1.90	1.02 $\pm$ 0.66	1.14–3.63	2.51 $\pm$ 1.10	0.14–0.34	0.25 $\pm$ 0.08	0.06–0.38	0.20 $\pm$ 0.16
downstream channel (n=5)	0.02–0.56	0.20 $\pm$ 0.23	0.15–1.61	0.67 $\pm$ 0.60	0.04–0.22	0.09 $\pm$ 0.74	0.19–0.36	0.28 $\pm$ 0.07
Farmland (n=3)	0.02–0.13	0.09 $\pm$ 0.06	0.16–2.53	1.14 $\pm$ 1.24	0.05–0.08	0.07 $\pm$ 0.02	0.12–1.81	0.71 $\pm$ 0.95
Background [28]	0.017–0.35	0.056	0.013–0.42	0.053	0.010–0.20	0.067	0.045–1.88	0.62
National average [29]	0.0018–0.52	0.038	0.0024–0.43	0.037	0.001–0.437	0.055	0.12–2.18	0.58

n: Sampling number

value and the national average value, they were far lower than the nuclides concentrations in the tailings reservoir. Concentrations of  $^{238}\text{U}$ ,  $^{226}\text{Ra}$  and  $^{232}\text{Th}$  decreased from upstream to downstream channel, suggesting that radionuclides accumulated in the sediment through the flow capture.  $^{226}\text{Ra}$  had the highest average activity concentrations of  $2.51 \text{ Bq g}^{-1}$  and  $^{40}\text{K}$  had the lowest average activity concentrations of  $0.20 \text{ Bq g}^{-1}$  in the sediments of upstream channel, being similar to the distribution patterns of nuclide concentrations in tailings reservoir.

Except for  $^{40}\text{K}$ , average concentrations of  $^{238}\text{U}$ ,  $^{226}\text{Ra}$  and  $^{232}\text{Th}$  in the farmland were lower than most of other sampling sites. The average activity concentrations of  $^{232}\text{Th}$  and  $^{40}\text{K}$  were  $0.07$  and  $0.71 \text{ Bq g}^{-1}$ , respectively. They were similar to the background value, while  $^{226}\text{Ra}$  concentrations were 21.51 times of the background value. It implies that the content of radon gas ( $^{226}\text{Ra}$  decaying daughter) may be high in this area.

### Migration of radionuclides

As can be seen from Fig. 2, radionuclide concentrations in the tailings reservoir were higher than in other regions away of tailings reservoir areas. The nuclide concentrations in the samples decreased with distance away from the reservoir area. Concentrations of  $^{238}\text{U}$  and  $^{226}\text{Ra}$  around the tailings reservoir were much higher than  $^{232}\text{Th}$  and  $^{40}\text{K}$ . In addition,  $^{238}\text{U}$  and  $^{226}\text{Ra}$  have similar distribution patterns (Fig. 2). At a distance of 250 m (*point 3-1*) the concentration of  $^{226}\text{Ra}$  from the tailings reservoir was  $3.63 \text{ Bq g}^{-1}$  and decreased to  $1.61 \text{ Bq g}^{-1}$  at 550 m (*point 4-1*) in the sediment downstream. There is a continuous decrease of  $^{238}\text{U}$  and  $^{226}\text{Ra}$  concentrations from 250 m (*point 3-1*) in the upstream of channel area to 610 m (*point 4-2*) in the downstream along

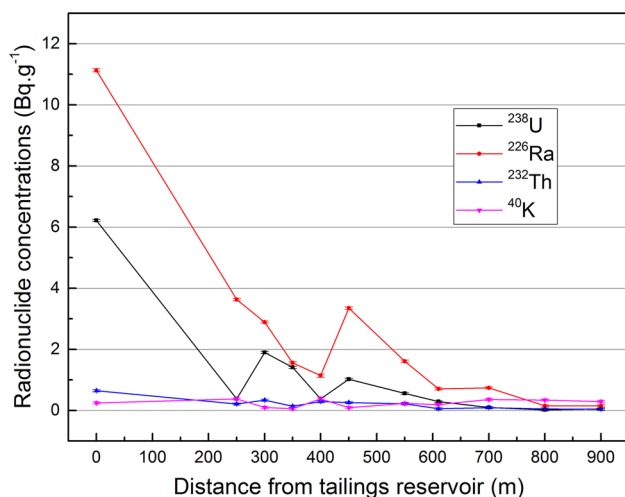


**Fig. 2** Concentrations of  $^{238}\text{U}$ ,  $^{226}\text{Ra}$ ,  $^{232}\text{Th}$  and  $^{40}\text{K}$  in soil and sediment samples around the tailings reservoir

the water flow except at 450 m (*point 3-4*). It shows that adsorption has a dominant role in controlling radionuclides distribution in the water–soil system [18]. Nevertheless, concentrations of  $^{238}\text{U}$  and  $^{226}\text{Ra}$  at a distance of 450 m suddenly increased, probably because the samples were taken from the upper sediment water which was a mixture of treated and percolated water. The nuclides in the water are easy to accumulate at this point and make the high concentration nuclides consequently. In addition, concentrations of  $^{232}\text{Th}$  around the tailings reservoir are relatively low and stable in general. This is due to the relatively low solubility of Th, which is generally transported with particulate matter and becomes deposited in water bodies [32]. Compared with  $^{238}\text{U}$ ,  $^{226}\text{Ra}$  and  $^{232}\text{Th}$ ,  $^{40}\text{K}$  had the lowest average activity concentrations of  $0.24 \text{ Bq g}^{-1}$  in the tailings reservoir and  $0.20 \text{ Bq g}^{-1}$  in the sediments of upstream channel, respectively. Furthermore,  $^{40}\text{K}$  had the minimum variability in the study area. They were all lower than the background value of Jiangxi province apart from the farm samples, which indicates that it has not been obviously affected by the tailings reservoir.

In order to ascertain influence extent of radionuclides in the tailings reservoir, the spatial distribution of  $^{238}\text{U}$ ,  $^{226}\text{Ra}$ ,  $^{232}\text{Th}$  and  $^{40}\text{K}$  were plotted by Kriging interpolation in Fig. 3. It shows that the spatial occurrence of  $^{238}\text{U}$ ,  $^{226}\text{Ra}$  and  $^{232}\text{Th}$  were similar, but the distribution pattern of  $^{40}\text{K}$  was different. It indicates that the concentrations of  $^{238}\text{U}$ ,  $^{226}\text{Ra}$  and  $^{232}\text{Th}$  are greatly affected by the tailings reservoir. However, the concentration of  $^{40}\text{K}$  was low near the tailings reservoir, while it was high in the southern farmland area. It suggests that the sources of  $^{40}\text{K}$  are different from other nuclides, which are not affected obviously by the tailings reservoir.

### Gross $\alpha$ , $\beta$ activity concentrations

The gross  $\alpha$  and  $\beta$  activity concentrations in the soil samples were determined by low background  $\alpha$  and  $\beta$  measuring instruments (Table 2). Figure 4 shows the variation of gross  $\alpha$  and  $\beta$  with distance from the tailings reservoir in soil and sediment samples.

Average values of gross  $\alpha$  and  $\beta$  in the uranium tailings sands were highest in the study area, which were  $51.35 \text{ Bq g}^{-1}$  and  $35.22 \text{ Bq g}^{-1}$ , respectively. The gross  $\alpha$  and  $\beta$  specific activity were 35 times and 27.5 times higher than values found in another decommissioned uranium mine area ( $1.46 \text{ Bq g}^{-1}$  for  $\alpha$ ,  $1.28 \text{ Bq g}^{-1}$  for  $\beta$ ) [33]. The high  $\alpha$  and  $\beta$  activity concentrations are due to the fact that most of the  $^{238}\text{U}$ ,  $^{232}\text{Th}$ ,  $^{226}\text{Ra}$  and their daughters emit  $\alpha$  rays, and a few of them emit  $\beta$  rays during decaying process. The average concentrations of gross  $\alpha$  and  $\beta$  in the tailings dam were  $2.31 \text{ Bq g}^{-1}$  and  $1.97 \text{ Bq g}^{-1}$ , respectively, showing the lowest values in the study area.

**Fig. 3** Concentrations distribution of radionuclide  $^{238}\text{U}$ ,  $^{226}\text{Ra}$ ,  $^{232}\text{Th}$ ,  $^{40}\text{K}$  in the study area. (a:  $^{238}\text{U}$ , b:  $^{226}\text{Ra}$ , c:  $^{232}\text{Th}$ , d:  $^{40}\text{K}$ )

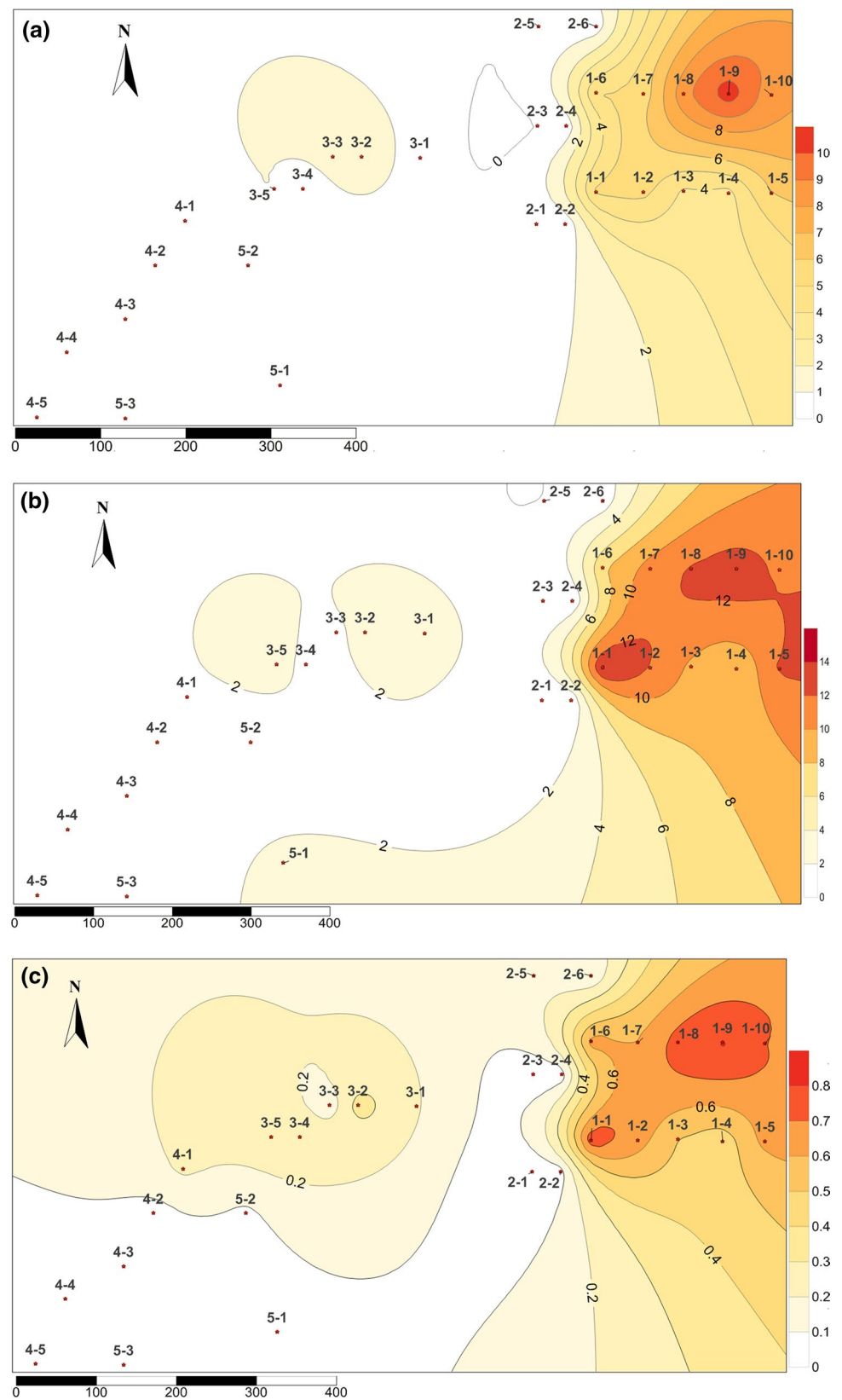
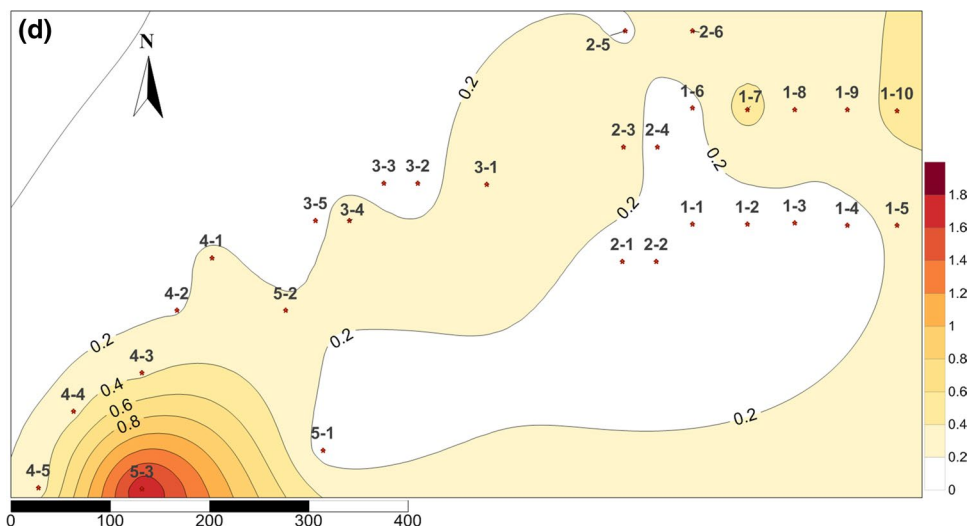


Fig. 3 (continued)



**Table 2** The statistics of gross  $\alpha$  and  $\beta$  specific activity in the soils and sediments

Sample area	Gross $\alpha$ ( $\text{Bq g}^{-1}$ )			Gross $\beta$ ( $\text{Bq g}^{-1}$ )		
	Range	Average $\pm$ SD	CV (%)	Range	Average $\pm$ SD	CV (%)
Tailings sand (n = 10)	76.19–33.12	51.35 $\pm$ 13.29	25.88	27.24–39.86	35.22 $\pm$ 1.40	12.52
Dam (n = 6)	0.55–9.61	2.31 $\pm$ 3.58	154.98	0.82–6.89	1.97 $\pm$ 2.41	122.34
upstream channel (n = 5)	10.76–29.88	19.89 $\pm$ 9.31	1.56	6.33–11.14	9.62 $\pm$ 2.11	21.93
downstream channel (n = 5)	0.62–19.17	5.33 $\pm$ 7.79	146.15	1.75–6.96	3.22 $\pm$ 2.41	74.84
Farmland (n = 3)	0.98–11.35	5.18 $\pm$ 5.46	105.41	0.82–6.02	3.55 $\pm$ 2.61	73.52
One decommissioned uranium mine [33]	1.09–2.12	1.46	N/A	0.97–1.84	1.28	N/A

n: Sampling number

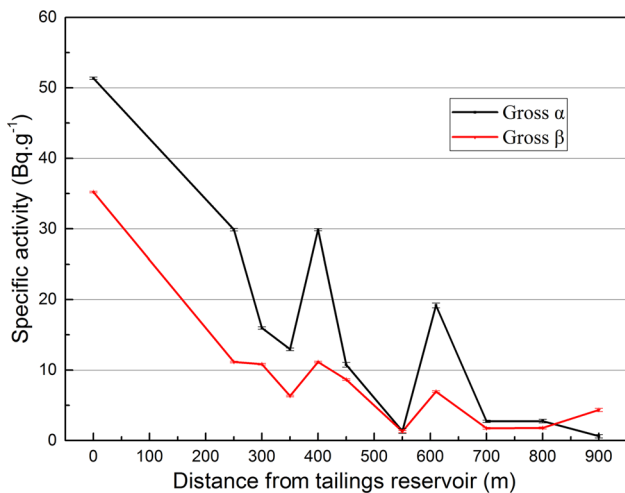


**Fig. 4** Gross  $\alpha$  and  $\beta$  specific activities in soil and sediment samples around the tailings reservoir

These values were similar to the levels of the decommissioned uranium mine area [33]. As can be seen in Fig. 4, gross  $\alpha$  and  $\beta$  activity had the same variation trends and  $\beta$

activity concentrations were lower than  $\alpha$  concentrations. It can be observed that the radioactivity level decreased with distance. Compared to radioactivity levels of the tailings reservoir and upstream channels, the gross  $\alpha$  and  $\beta$  concentrations in the sediment of downstream channel were reduced by an order of magnitude.

Coefficient of variation (CV) reflects the degree of discretion and spatial variation. As shown in Table 2, the gross  $\alpha$  specific activities varied greatly in samples collected from the dam, the downstream of channel sediment and farmland, while the  $\beta$  specific showed a great change in samples collected from the dam. The low CV in the uranium sand samples illustrates that the variations of gross  $\alpha$  activity were relatively moderate in the uranium tailings reservoir, but the coefficient of variation in the sediment of upstream channel was 1.56%, showing that the variations are weak. The variations of gross  $\beta$  activity were relatively moderate except in the dam. These results suggested that the distributions of  $\alpha$  and  $\beta$  specific activity were uneven and displayed a certain fluctuation in different areas around uranium tailings reservoir, which was caused by the influences of uranium tailings, fertilization, farming and human activities.

## Correlation analysis

To identify the relationship between nuclides around the tailings reservoir, correlation analyses were done between radionuclides pairs, as shown in Table 3. Concentrations of  $^{226}\text{Ra}$  were significantly positively correlated with  $^{238}\text{U}$ , because  $^{226}\text{Ra}$  is one of daughter of  $^{238}\text{U}$ . Moreover, concentrations of  $^{238}\text{U}$  were significantly positively correlated with  $^{226}\text{Ra}$  and  $^{232}\text{Th}$  with the Pearson coefficients (PC) both greater than 0.9. This is due to the fact that they are dissolved in soil under similar conditions and originate from similar reservoir rocks.  $^{232}\text{Th}$  concentration was significantly positively correlated with  $^{226}\text{Ra}$ . Similar cases have been reported in a previous study [7, 32]. However, PC between  $^{40}\text{K}$  and other three radionuclides was relatively small. It indicates that source of  $^{40}\text{K}$  is different from  $^{238}\text{U}$ ,  $^{226}\text{Ra}$  and  $^{232}\text{Th}$ . This is consistent with the result of characteristics of their spatial distribution. In addition,  $\alpha$  and  $\beta$  activity concentrations were positively significantly correlated with  $^{238}\text{U}$ ,  $^{226}\text{Ra}$  and  $^{232}\text{Th}$ , and PC values were about 0.9. It further confirms that  $\alpha$  and  $\beta$  rays are mainly derived from the  $^{238}\text{U}$ ,  $^{226}\text{Ra}$  and  $^{232}\text{Th}$  in the tailings reservoir.

## The radiation level assessment

Table 4 presents the absorbed dose rates in air at height of 1 m above the ground level around tailings reservoir. It can be seen that the gamma absorbed dose rates varied from 54 to 5369 nGy h<sup>-1</sup> with an average of 867 nGy h<sup>-1</sup> in study area. The average calculated gamma absorbed dose rates in this area was about 15 times higher than the worldwide average value (59 nGy h<sup>-1</sup>) [35], and 12 times of the background value of Jiangxi Province (73 nGy h<sup>-1</sup>) [28]. The lowest absorbed dose rate was found in the sediments of downstream channel and the highest value was found in uranium tailings reservoir. The gamma absorbed dose rates ranged from 1981 to 5369 nGy h<sup>-1</sup> with an average of 3274 nGy h<sup>-1</sup> in the uranium tailings reservoir. The average value was about 52 times higher than the average value in China (63 nGy h<sup>-1</sup>) [34], and 55 times higher than the worldwide average value (59 nGy h<sup>-1</sup>). It shows that the absorbed

**Table 4** The absorbed dose rates in air at height of 1 m above the ground level around tailings reservoir

Sample area	Absorbed dose rate/ (nGy h <sup>-1</sup> )	
	Range	Average
Tailings sand	1981–5369	3274
Dam	61–291	158
Sediment of upstream channel	367–1087	629
Sediment of downstream channel	54–401	162
Farmland	107–117	110
Background value [28]	14–341	73
Average in China [34]	N/A	63
Global average [35]	N/A	59

dose rates in the tailings reservoir were much larger than the background level and the average level in China. The high gamma absorbed dose rate in the uranium tailings reservoir was caused by the high concentrations of Th and U. The contribution of  $^{232}\text{Th}$  and  $^{238}\text{U}$  in the absorbed dose rate was calculated to be 19% and 81% in the uranium tailings reservoir, respectively; while contribution of  $^{40}\text{K}$  was 0.2%. Similar results have been obtained by in the Mandena deposit, South Madagascar [36]. The average gamma absorbed dose rate in the sediment of upstream channel was 629 nGy h<sup>-1</sup>, which is about 10 times higher than the average value in China, while the average gamma absorbed dose rates in the tailings dam and the sediment of downstream channel were about twice lower than the average value in China. In summary, the study area may be categorized as an area with a higher radiation level than the natural background.

## Conclusions

The present paper investigated the distribution and migration of radionuclides around a tailings reservoir in southern China. The results showed that, among the 5 sampling regions, the highest concentrations of  $^{238}\text{U}$ ,  $^{226}\text{Ra}$ , and  $^{232}\text{Th}$  all were distributed in the tailings sand samples, which were

**Table 3** The correlation coefficients of radionuclides in the study area

	$^{238}\text{U}$	$^{226}\text{Ra}$	$^{232}\text{Th}$	$^{40}\text{K}$	Gross $\alpha$	Gross $\beta$
$^{238}\text{U}$	1					
$^{226}\text{Ra}$	0.9263**	1				
$^{232}\text{Th}$	0.9427**	0.9653**	1			
$^{40}\text{K}$	-0.0870	-0.0947	-0.1246	1		
Gross $\alpha$	0.8455**	0.9435**	0.9301**	-0.1332	1	
Gross $\beta$	0.9363**	0.9785**	0.9687**	-0.0935	0.9494**	1

\*\* $P < 0.01$

\*\*Significant correlation at the 0.01 level



much higher than the background value and the national average value. It indicated that there was radioactive residue in the tailings reservoir, and it was a potential radioactive source. However, the highest concentrations of  $^{40}\text{K}$  was in samples from the farmland. Because  $^{238}\text{U}$ ,  $^{232}\text{Th}$ ,  $^{226}\text{Ra}$  and their daughters emitted  $\alpha$  and  $\beta$  rays during decaying process, the gross  $\alpha$  and  $\beta$  activity concentrations were high in the tailings reservoir. Furthermore, activity concentrations of  $\alpha$ ,  $\beta$  were positively correlated with  $^{238}\text{U}$ ,  $^{226}\text{Ra}$  and  $^{232}\text{Th}$  concentrations, with Pearson coefficient values being about 0.9. In addition, the gamma absorbed dose rates around tailings reservoir varied from 54 to 5369 nGy h<sup>-1</sup> with an average value of 867 nGy h<sup>-1</sup>. The high gamma absorbed dose rates in the uranium tailings reservoir may be caused by the high concentrations of  $^{232}\text{Th}$  and  $^{238}\text{U}$ . Because of the reduction of  $^{238}\text{U}$  and  $^{232}\text{Th}$  concentrations in the farmland, the average gamma absorbed dose rate reduced to less than twice of the national average value.

**Acknowledgements** This work was financially supported by the National Natural Science Foundation of China (Nos. 41502235, 41362011, 41662015); the Science and Technology Project of the Education Office of Jiangxi Province, China (GJJ160572).

## References

- Craft ES, Abu-Qare AW, Flaherty MM, Garofolo MC, Rincavage HL, Abou-Donia MB (2004) Depleted and natural uranium: chemistry and toxicological effects. *J Toxicol Environ Health* 7:297–317
- IAEA (2004) The long term stabilization of uranium mill tailings. TECDOC-1403, Vienna
- Abdelouas A (2006) Uranium mill tailings: geochemistry, mineralogy, and environmental impact. *Elements* 2(6):335–341
- Sethy NK, Jha VN, Sutar AK, Rath P, Sahoo SK, Ravi PM, Tripathi RM (2014) Assessment of naturally occurring radioactive materials in the surface soil of uranium mining area of Jharkhand, India. *J Geochem Explor* 142:29–35
- Bossey P, Gastberger M, Gohlh H, Hofer P, Hubmer A (2004) Vertical distribution of radionuclides in soil of a grassland site in Chernobyl exclusion zone. *J Environ Radioact* 73:87–99
- Foulkes M, Millward G, Henderson S, Blake W (2017) Bioaccessibility of U, Th and Pb in solid wastes and soils from an abandoned uranium mine. *J Environ Radioact* 173:85–96
- Yan X, Luo XG (2015) Radionuclides distribution, properties, and microbial diversity of soils in uranium mill tailings from south-eastern China. *J Environ Radioact* 139:85–90
- Bunzl K, Kretner R, Szeles M, Winkler R (1994) Transect survey of  $^{238}\text{U}$ ,  $^{228}\text{Ra}$ ,  $^{226}\text{Ra}$ ,  $^{210}\text{Pb}$ ,  $^{137}\text{Cs}$  and  $^{40}\text{K}$  in an agricultural soil near an exhaust ventilating shaft of a uranium mine. *Sci Total Environ* 149(3):225–232
- Charro E, Moyano A (2017) Soil and vegetation influence in plants natural radionuclides uptake at a uranium mining site. *Radiat Phys Chem* 141:200–206
- Mohammed SA, Mohamad SJ, Norlaili AK, Nisar A (2015) Distribution of  $^{226}\text{Ra}$ ,  $^{232}\text{Th}$ , and  $^{40}\text{K}$  in rice plant components and physicochemical effects of soil on their transportation to grains. *J Radiat Res Appl Sci* 8(3):300–310
- Rosén K, Vinichuk M (2014) Potassium fertilization and  $^{137}\text{Cs}$  transfer from soil to grass and barley in Sweden after the Chernobyl fallout. *J Environ Radioact* 130:22–32
- Elango L, Brindha K, Kalpana L, Sunny F, Nair R, Murugan R (2012) Groundwater flow and radionuclide decay-chain transport modelling around a proposed uranium tailings pond in India. *Hydrogeol J* 4(20):797–812
- Corcho AJA, Balsiger B, Rollin S, Jakob A, Burger M (2014) Radioactive and chemical contamination of the water resources in the former uranium mining and milling sites of Mailuu Suu (Kyrgyzstan). *J Environ Radioact* 138:1–10
- Winde F, Van der Walt IJ (2004) The significance of groundwater–stream interactions and fluctuating stream chemistry on waterborne uranium contamination of streams—a case study from a gold mining site in South Africa. *J Hydrol* 287:178–196
- Uralbekov BM, Smodis B, Burkitbayev M (2011) Uranium in natural waters sampled within former uranium mining sites in Kazakhstan and Kyrgyzstan. *J Environ Radioact* 289:805–810
- Laisaoui A, Mas JL, Hurtado S, Ziad N, Villa M, Benmansour M (2013) Radionuclide activities and metal concentrations in sediments of the Sebou Estuary, NW Morocco, following a flooding event. *Environ Monit Assess* 185:5019–5029
- Carvalho FP, Oliveira JM, Lopes I, Batista A (2007) Radionuclides from past uranium mining in rivers of Portugal. *J Environ Radioact* 98(3):298–314
- Kayzar TM, Villa AC, Lobaugh ML, Gaffney AM, Williams RW (2014) Investigating uranium distribution in surface sediments and waters: a case study of contamination from the Juniper Uranium Mine, Stanislaus National Forest, CA. *J Environ Radioact* 136:85–97
- Zhang L, Liu ZR (2018) Pollution characteristics and risk assessment of uranium and heavy metals of agricultural soil around the uranium tailing reservoir in Southern China. *J Radioanal Nucl Chem* 318:923–933
- Mathuthu M, Dlamini SG, Njinga RL (2018) Exposure risks assessment due to gamma emitting radionuclides in soils and consumable waters around princess gold mine dump in roodepoort, South Africa. *Mine Water Environ* 37(1):98–105
- Déjeant A, Galois L, Roy R, Calas G, Boekhout F, Phrommavanh V, Descostes M (2016) Evolution of uranium distribution and speciation in mill tailings, COMINAK Mine, Niger. *Sci Total Environ* 545–546:340–352
- Chautard C, Beaucaire C, Gérard M, Phrommavanh V, Nos J, Galois L, Calas G, Roy R, Descostes M (2017) Geochemical characterization of U tailings (Bois Noirs Limouzat, France). *Procedia Earth Planet Sci* 17:308–311
- General Administration of Quality Supervision, Inspection and Quarantine of the People's Republic of China, China National Standardization Administration (2014) Determination of radionuclides in soil by gamma spectrometry, GB/T 11743–2013. China Standard Press, Beijing
- Adukpo OK, Faanu A, Lawlubi H, Tettey-Larbi L, Emi-Reynolds G, Darko EO, Kansaana C, Kpeglo DO, Awudu AR, Glover ET, Amoah PA, Efa AO, Agyemang LA, Agyeman BK, Kpordzro R, Doe AI (2015) Distribution and assessment of radionuclides in sediments, soil and water from the lower basin of river Pra in the Central and Western Regions of Ghana. *J Radioanal Nucl Chem* 303(3):1679–1685
- General Administration of Quality Supervision, Inspection and Quarantine of the People's Republic of China, China National Standardization Administration (2008) Low background alpha and/or beta measuring instruments, GB/T 11682-2008. China Standard Press, Beijing
- Beck HL, Decompo J, Gogolak G (1972) In-situ Ge (Li) and NaI (Ti) Gamma-ray spectrometry. USAEC. HASL-258

27. International Commission on Radiation Units and Measurements (ICRU) (1994) Gamma-ray spectrometry in the environment. ICRU Report 53. Washington DC, USA
28. Li XD, Zheng SH, Wu XR, Li Y, Sun XR, Yang MZ, Wan M, Zhang SM (1993) Investigation of natural radionuclide contents in soil in Jiangxi Province. *Radiat Prot* 4:291–294
29. Cao LS, Yang YX, Zhang Y, Zheng YM, Yang T (2012) Distribution pattern of radionuclides in the soil of mainland china. *J East China Inst Technol (Nat Sci)*. <https://doi.org/10.3969/j.issn.1674-3504.2012.02.011>
30. Jiang JQ, Lao YJ, Wang L, Qi W, Gao B, Yao GY (2015) Vertical distribution characteristics of nuclide in shallow tailings of uranium mine tailings reservoir area. *Environ Chem* 34(8):1561–1563
31. Seeley FG (1977) Problem in the separation of Ra from uranium ore tailings. *Hydrometallurgy* 2:249
32. Prasad NGS, Nagaiah N, Ashok GV, Karunakara N (2008) Concentrations of  $^{226}\text{Ra}$ ,  $^{232}\text{Th}$ , and  $^{40}\text{K}$  in the soils of Bangalore region, India. *Health Phys* 94:264–271
33. Mou S, Wu GL, Yang ZJ, Tang L, Zhang BX, Huang RQ, Kuang JY (2016) Investigation on gross  $\alpha$  and  $\beta$  radioactivity level in the surrounding environment of a decommissioned uranium mine. *Chin J Radiol Health* 25(5):581–584
34. Pan ZQ, Guo MQ, Cui GZ, Yang Y (1992) Estimation of natural radiation background level and population dose in China. *Radiat Prot* 12(4):251–259
35. UNSCEAR (2000) Sources and effects of ionizing radiation. United Nations Scientific Committee on the Effects of Atomic Radiation. United Nation, New York
36. Hao DV, Dinh CN, Jodlowski P, Kovacs T (2019) High-level natural radionuclides from the Mandena deposit, South Madagascar. *J Radioanal Nucl Chem* 319(3):1331–1338

**Publisher's Note** Springer Nature remains neutral with regard to jurisdictional claims in published maps and institutional affiliations.